Parametrically driven surface waves on viscous ferrofluids

Hanns Walter Müller
Institut für Theoretische Physik, Universität des Saarlandes, D-66041 Saarbrücken, Germany
(Received 24 April 1998)

Standing waves on the surface of a ferrofluid in a normal magnetic field can be excited by a vertical vibration of the container. A stability theory for the onset of these parametrically driven waves is developed, taking viscous dissipation and finite depth effects into account. It will be shown that a careful choice of the filling level permits the normal and anomalous dispersion branches to be measured. Furthermore it will be demonstrated that the parametric driving mechanism may lead to a delay of the Rosensweig instability. A bicritical situation can be achieved when Rosensweig and Faraday waves interact. [S1063-651X(98)05311-2]

PACS number(s): 47.20.Ma, 75.50.Mm

I. INTRODUCTION

A wide application spectrum of ferrofluids is based on the free surface behavior in the presence of a magnetic field [1–3]. Cowley and Rosensweig [4] found that the surface undergoes a spontaneous instability in a static normal magnetic field. As the instability is also static, a theoretical description of the onset can be based on the dispersion relation $\omega_0(k)$ for *inviscid* surface waves. As soon as the applied magnetic field exceeds a critical threshold, ω_0^2 becomes negative and a stationary surface pattern (e.g., in the form of hexagons) develops. For magnetic fields slightly below the Rosensweig threshold the dispersion $\omega_0(k)$ is nonmonotonous with an intermediate branch of negative slope (anomalous dispersion). Although there is experimental evidence [5,6] of this hysteretic behavior, the anomalous dispersion branch has not been directly detected yet. Recently, a twomodal nonlinear surface pattern, denoted as ''twin peaks'' has been observed [6], which might be the result of a bicritical situation with two competing unstable wave numbers.

The excitation of surface waves can be realized by different mechanisms. For instance, a horizontal vibration of the vessel [7] or a modulated air jet directed against the surface [5] provide a driving force which couples additively to the equations of motion: No matter how small the excitation amplitude, it always leads to a wave excitation. This is in contrast to the multiplicative (parametric) forcing, where wave generation is successful only beyond a finite excitation amplitude. That way surface waves have been excited by a modulation of the applied magnetic field [8–10] or by a vertical vibration of the vessel [6].

In principle, different excitation mechanisms may result in distinct wave dispersions. However, in case of weak dissipation (which frequently applies to surface wave experiments) the necessary driving forces remain small and, thus, the dispersion approximately coincides with that of *free inviscid* surface waves. Nevertheless, viscous dissipation can be incorporated into the theory. Such computations have been performed [11,12] for *free* surface waves. No investigation has yet been undertaken for surface waves in the presence of a parametric drive.

The present study will fill this gap. It will be shown that, depending on the filling depth h, a more or less extended region of available wave numbers can be gradually eliminated from the spectrum of unstable modes. By virtue of this effect a specific experiment will be proposed by which all dispersion branches, including the anomalous one, can be measured. The theory outlined below will also demonstrate that the parametric drive can be used to delay or suppress the Rosensweig instability until it intersects with the Faraday instability. Nonlinear wave number resonance in the neighborhood of this bicritical situation is expected to induce interesting surface wave pattern formation.

II. THE SYSTEM

A horizontally unbounded ferrofluid layer of thickness h is exposed to a dc magnetic field perpendicular to its free surface (see Fig. 1 for a sketch). The ferrofluid is sandwiched between a covering air layer (medium 1) and the magnetically impermeable container material (medium 3). Quantities with superscripts in parenthesis refer to these media. For brevity, variables without superscript denote the ferrofluid.

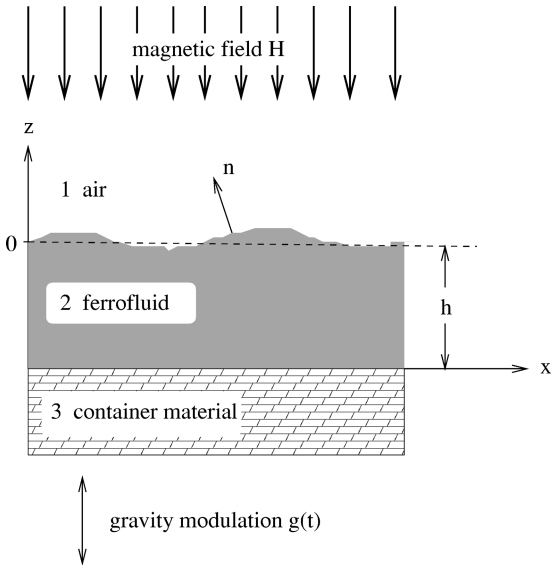

FIG. 1. Sketch of the setup. A ferrofluid layer of infinite horizontal extension is exposed to a static normal magnetic field and a time dependent gravity modulation $g(t)$ directed along the vertical z axis. The container material below the fluid and the covering air are magnetically impermeable.

In order to excite surface waves the whole apparatus is exposed to a vertical vibration [effective gravity modulation $g(t)$].

A. Hydrodynamic equations and boundary conditions

The fluid motion is governed by the hydrodynamic field equations. For a constant density fluid, with a velocity field $\mathbf{v}(\mathbf{r},t)=(u,v,w)$ the balance equations for mass and linear momentum read as

$$\boldsymbol{\nabla}\cdot\mathbf{v}=0, \tag{2.1}$$

$$\rho(\partial_t\mathbf{v}+\mathbf{v}\cdot\boldsymbol{\nabla})\mathbf{v}=\boldsymbol{\nabla}\cdot\sigma-\rho g(t)\mathbf{e}_z, \tag{2.2}$$

$$\sigma_{ij}=-p\,\delta_{ij}+\eta(\boldsymbol{\nabla}_i v_j+\boldsymbol{\nabla}_j v_i)-\frac{\mu_0(1+\chi)}{2}H^2\delta_{ij}+H_iB_j. \tag{2.3}$$

The stress tensor σ consists of the pressure $p(\mathbf{r},t)$, a viscous term proportional to the dynamic viscosity η, and two electromagnetic contributions. The latter ones result from the Maxwell stress tensor with the magnetic field $\mathbf{H}$, the induction $\mathbf{B}=\mu_0(\mathbf{H}+\mathbf{M})$, and the magnetization $\mathbf{M}$. Magnetostriction has been neglected. Furthermore ρ is the density of the fluid and $g(t)$ is the time dependent acceleration corresponding to the vertical vibration of the system.

The equations of motion have to be supplemented by appropriate boundary conditions. At the bottom of the container at $z=-h$ the no-slip condition applies

$$\mathbf{v}|_{-h}=0. \tag{2.4}$$

To describe waves at the surface of the layer we introduce the surface elevation $\zeta(x,y,t)$, which vanishes when the fluid is in its unperturbed base state (undeformed plane surface). The kinematic relation between ζ and the velocity field reads as

$$\partial_t\zeta+u|_\zeta\partial_x\zeta+v|_\zeta\partial_y\zeta=w|_\zeta, \tag{2.5}$$

where $|_\zeta$ stands for the evaluation at the free surface. From the force balance at the free surface $z=\zeta(x,y,t)$ we get

$$(\sigma^{(1)}-\sigma)|_\zeta\cdot\mathbf{n}=\gamma(\boldsymbol{\nabla}\cdot\mathbf{n})\mathbf{n}, \tag{2.6}$$

where $\mathbf{n}=(-\partial_x\zeta,-\partial_y\zeta,1)/\sqrt{1+(\partial_x\zeta)^2+(\partial_y\zeta)^2}$ is the local surface normal vector and γ the surface tension. Due to the small dynamic viscosity of air, viscous friction therein can be neglected and the stress tensor is well approximated by

$$\sigma^{(1)}_{ij}=-\left[p_{atm}-\frac{\mu_0}{2}(H^{(1)})^2\right]\delta_{ij}$$

with the constant atmospheric pressure p_{atm}.

B. The electromagnetic equations and boundary conditions

For hydrodynamic problems of nonconducting ferrofluids Maxwell's equations can be taken in their magnetostatic approximation [1]

$$\boldsymbol{\nabla}\times\mathbf{H}^{(i)}=0,\quad \boldsymbol{\nabla}\cdot\mathbf{B}^{(i)}=0,\quad i=1,2,3. \tag{2.7}$$

At the top and bottom interface of the ferrofluid the tangential component of $\mathbf{H}$ and the normal component of $\mathbf{B}$ have to be continuous

$$\mathbf{n}\cdot(\mathbf{B}^{(1)}-\mathbf{B})|_\zeta=0,\quad \mathbf{e}_z\cdot(\mathbf{B}-\mathbf{B}^{(3)})|_{-h}=0, \tag{2.8}$$

$$\mathbf{n}\times(\mathbf{H}^{(1)}-\mathbf{H})|_\zeta=0,\quad \mathbf{e}_z\times(\mathbf{H}-\mathbf{H}^{(3)})|_{-h}=0. \tag{2.9}$$

C. The basic state and linearized equations of motion

When the container of the fluid is subject to a vertical oscillatory displacement with frequency 2Ω, the earth gravity g_0 is modulated in the comoving frame according to $g(t)=g_0+a\cos(2\Omega t)$. As long as the modulation amplitude a is small, the system is in its basic or ground state. In a container-fixed frame of reference the fluid rests ($\mathbf{v}=0$) and the surface is perfectly flat ($\zeta=0$). The magnetic properties inside and outside the fluid are stationary and spatially homogeneous $\mathbf{H}^{(i)}=\mathbf{H}^{(i)}_G=H^{(i)}_G\mathbf{e}_z$, $\mathbf{M}=\mathbf{M}_G=M_G\mathbf{e}_z$, where the subscript G refers to the ground state. When $\mathbf{v}=0$ the time dependent drive in the Navier-Stokes equation is compensated by the pressure

$$p_G(\mathbf{r},t)=p_{atm}-\frac{\mu_0}{2}M_G^2-\rho g(t)z. \tag{2.10}$$

The second term in Eq. (2.10) is the magnetic pressure jump at the free surface.

If the mechanical excitation is strong enough the ground state becomes unstable and surface waves develop. Let us denote deviations from the basic state profiles by

$$\mathbf{v},\quad \zeta,\quad \delta p=p-p_G,\quad \mathbf{m}=\mathbf{M}-\mathbf{M}_G,\quad \mathbf{h}^{(i)}=\mathbf{H}^{(i)}-\mathbf{H}^{(i)}_G. \tag{2.11}$$

After linearizing the magnetohydrodynamic equations and boundary conditions one obtains for the ferrofluid bulk

$$\boldsymbol{\nabla}\cdot\mathbf{v}=0, \tag{2.12}$$

$$\rho\partial_t\mathbf{v}=-\boldsymbol{\nabla}\delta p+\eta\nabla^2\mathbf{v}+\mu_0\boldsymbol{\nabla}(\mathbf{M}_G\cdot\mathbf{h}). \tag{2.13}$$

On taking the curl curl of Eq. (2.13) the gradient terms are eliminated and an equation for the vertical component w of the velocity field results

$$(\partial_t-\nu\nabla^2)\nabla^2 w=0, \tag{2.14}$$

where $\nu=\eta/\rho$ is the kinematic viscosity. At the bottom of the vessel the no-slip boundary conditions read as

$$w|_{-h}=\partial_z w|_{-h}=0, \tag{2.15}$$

while one gets at the free surface

$$\partial_t\zeta=w|_0, \tag{2.16}$$

$$(\partial_z^2-\nabla_\perp^2)w|_0=0, \tag{2.17}$$

$$\{-\rho\partial_t\partial_z w+\eta\partial_z^3 w+3\,\eta\partial_z\nabla_\perp^2 w+\rho g(t)\nabla_\perp^2\zeta-\gamma\nabla_\perp^4\zeta - \mu_0 M_G\nabla_\perp^2[(\mathbf{h}+\mathbf{m})\cdot\mathbf{e}_z]\}|_0=0. \tag{2.18}$$

Here $|_0$ denotes evaluation at the resting free surface and $\nabla_\perp=(\partial_x,\partial_y,0)$ is the horizontal gradient. From the fourth term in Eq. (2.18) it can be seen that the drive mechanism is parametric.

The magnetic fields obey

$$\nabla\times\mathbf{h}^{(i)}=0,\quad \nabla\cdot\mathbf{h}^{(i)}=0,\quad i=1,3 \tag{2.19}$$

$$\nabla\times\mathbf{h}=0,\quad \nabla\cdot(\mathbf{h}+\mathbf{m})=0 \tag{2.20}$$

with the boundary conditions

$$\mathbf{e}_z\cdot(\mathbf{h}+\mathbf{m}-\mathbf{h}^{(1)})|_0=0,\quad \mathbf{e}_z\cdot(\mathbf{h}+\mathbf{m}-\mathbf{h}^{(3)})|_{-h}=0, \tag{2.21}$$

$$\begin{Bmatrix}\mathbf{e}_x\\ \mathbf{e}_y\end{Bmatrix}\cdot\{M_G\nabla_\perp\zeta-(\mathbf{h}-\mathbf{h}^{(1)})|_0\}=0,\quad \begin{Bmatrix}\mathbf{e}_x\\ \mathbf{e}_y\end{Bmatrix}\cdot(\mathbf{h}-\mathbf{h}^{(3)})_{-h}=0. \tag{2.22}$$

III. SURFACE WAVES

In the absence of driving $[g(t)=g_0=\text{const}]$ we denote surface waves as ''free.'' In this case the stability problem is autonomous in time and a solution of the form $\zeta\propto e^{i(kx+\omega t)}$ applies. The vertical dependencies of the fields can be integrated and the boundary conditions yield a solvability condition, which determines the dispersion $\omega(k)$.

A. Inviscid free surface waves

For an ideal fluid ($\eta=0$) the solvability condition yields the dispersion of inviscid free surface waves

$$-\omega^2+\omega_0^2(k)=0, \tag{3.1}$$

$$\omega_0^2(k)=\tanh(kh)\left\{g_0k-\frac{\mu_0}{\rho}\frac{1+\chi}{2+\chi}\times\left(1-\frac{2\chi}{(2+\chi)^2e^{2kh}-\chi^2}\right)M_G^2k^2+\frac{\gamma}{\rho}k^3\right\}. \tag{3.2}$$

This result has been derived earlier by several authors [8,11,12]. Equation (3.2) holds for a constant susceptibility magnetic fluid with $\mathbf{M}=\chi\mathbf{H}$. If the magnetization approaches saturation this approximation ceases to apply. Then the magnetic contribution in (3.2) has to be replaced by

$$-\frac{\mu_0}{\rho}\frac{1+\overline{\chi}}{2+\overline{\chi}}\left(1-\frac{2\overline{\chi}}{(2+\overline{\chi})^2e^{2kh(1+\chi)/(1+\chi)}-\overline{\chi}^2}\right)M_G^2k^2, \tag{3.3}$$

where $\chi=\partial M/\partial H|_{H_G}$ is the differential susceptibility, $\tilde{\chi}=M_G/H_G$ the chord susceptibility and $1+\overline{\chi}=\sqrt{(1+\chi)(1+\tilde{\chi})}$. For the results presented in Sec. VI the approximation (3.2) is sufficient.

As the magnetic term in Eq. (3.2) opposes to gravity and surface tension, the dispersion may become nonmonotonous as a function of the wave number k. If the magnetization M_G is sufficiently strong, ω_0^2 changes sign and the normal field or Rosensweig instability occurs. Note: as this instability is *static* the expressions for the critical magnetization and the critical wave numbers

$$M_R^2=\frac{2}{\mu_0}\frac{2+\overline{\chi}}{1+\overline{\chi}}\sqrt{\rho g_0\gamma},\quad k_R=\left(\frac{\rho g_0}{\gamma}\right)^{1/2} \tag{3.4}$$

apply for inviscid as well as viscous fluids. Equation (3.4) holds in the deep water limit $kh\gg1$. The h dependence of M_R and k_R has been investigated by Weilepp and Brand [11] and Abou *et al.* [12]. Figure 2 depicts the inviscid dispersion (3.2) for three different filling levels at a magnetization $M_G=0.99\times M_R$, i.e., 1% below the Rosensweig threshold for a deep fluid layer.

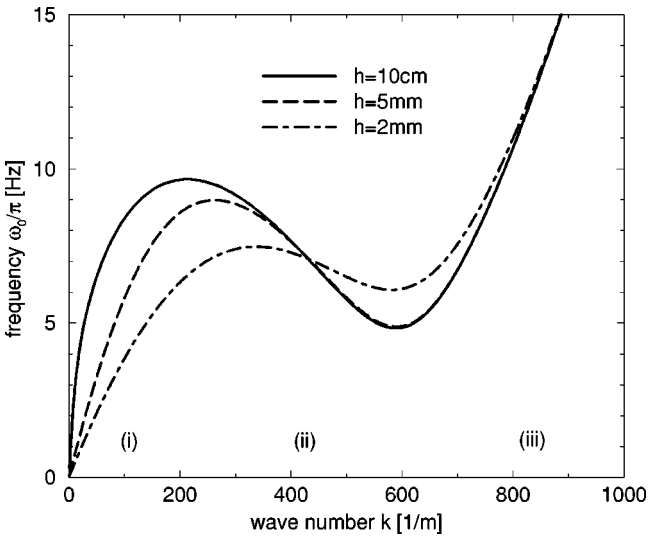

FIG. 2. The inviscid dispersion relation [Eq. (3.2)] for free surface waves at different filling levels h. The applied magnetic field is only 1% below the Rosensweig threshold M_R giving a strong hysteresis. The two normal branches are labeled by (i) and (iii), the anomalous branch with negative slope by (ii). Fluid parameters are for EMG 909 (Ferrofluidics corporation): $\nu=6$ mm^2/s, $\rho=1.02$ g/cm^3, $\gamma=0.0265$ N/m, and $\chi=0.8$.

B. Viscous free surface waves

It is important to note that the hydrodynamic bulk equations and boundary conditions [Eqs. (2.12), (2.14)–(2.17)] for w can be solved in terms of ζ without reference to the magnetic properties of the fluid. Likewise, the solution of the magnetic-field equations and boundary conditions [Eqs. (2.19)–(2.22)] can be expressed by ζ without knowledge of the velocity field w. Velocity and magnetic fields are coupled by the normal force balance (2.18). Consequently the viscous contributions therein can be overtaken from *nonmagnetic* fluids. Invoking the expression of Kumar and Tuckerman [13] the viscous dispersion reads as

$$-\omega^2+\omega^2X(k,\omega)+\omega_0^2(k)=0, \tag{3.5}$$

where

$$-\omega^2+\omega^2 X(k,\omega)=\frac{\nu^2}{q\coth(qh)-k\coth(kh)}$$
$$\times\left\{q[4k^4+(k^2+q^2)^2]\coth(qh)-k[4k^2q^2+(k^2+q^2)^2]\tanh(kh)-\frac{4k^2q(k^2+q^2)}{\cosh(kh)\sinh(qh)}\right\} \quad (3.6)$$

and $q=\sqrt{k^2+i\omega/\nu}$. This expression has recently been reproduced by Abou *et al.* [12]. Note their complicated representation of $\omega_0^2(k)$ coincides with Eq. (3.2). Usually for surface wave experiments the limit of weak dissipation applies, where the dimensionless parameter $\nu k^2/\omega$ is small. On expanding Eq. (3.6) up to first order one gets

$$X(k,\omega)=(-1+i)\frac{\sqrt{2}}{\sinh(2kh)}\left(\frac{\nu k^2}{\omega}\right)^{1/2}$$
$$+i[3+\coth^2(kh)]\left(\frac{\nu k^2}{\omega}\right)+O\left(\frac{\nu k^2}{\omega}\right)^{3/2}. \quad (3.7)$$

The first term results from the viscous boundary layer along the bottom of the container [14] and contributes appreciably only if $kh\lesssim 1$. It dies out rapidly when the wavelength falls short of the depth h. In that case the second term in Eq. (3.7) dominates. It is proportional to νk^2 and reflects viscous dissipation in the bulk of the fluid. By varying the filling level h the relation between bulk and bottom damping is under external control.

C. Parametrically driven surface waves

For time dependent gravity $g(t)$ the boundary condition (2.18) is no longer autonomous in time. The parametric drive couples neighboring temporal Fourier modes. At the onset of the instability the monochromatic time dependence $e^{ikx+\omega t}$ must be replaced by the Floquet ansatz

$$\zeta\propto e^{i\beta\Omega t}\sum_{n=-\infty}^{\infty}\zeta_n e^{2in\Omega t}. \quad (3.8)$$

Substitution of this ansatz leads to the infinite dimensional tridiagonal system

$$\{-\omega^2+\omega^2X(k,\omega)+\omega_0^2\}\zeta_n+\frac{ak\tanh(kh)}{2}(\zeta_{n+1}+\zeta_{n-1})=0, \quad (3.9)$$

where $\omega=(2n+\beta)\Omega$. The case $\beta=1$ ($\beta=0$) corresponds to the subharmonic (harmonic) surface response. The Eqs. (3.9) can be numerically approximated by an appropriate cutoff (see Ref. [13] for details). The solvability condition yields the neutral stability curves $a^{(S)}(k)$ and $a^{(H)}(k)$ for the subharmonic (S) and the harmonic (H) surface resonance, respectively. A subsequent minimization with respect to the wave number determines the critical onset amplitudes $a_c^{(S)}$ and $a_c^{(H)}$ and the critical wave numbers k_S, k_H. These quantities can be investigated as a function of the driving frequency Ω and the dc component of the magnetic field H_G.

IV. RESULTS

A. Dispersion for parametrically excited surface waves

In this section we discuss the onset $a_c^{(S)}(\Omega)$ and the dispersion $k_S(\Omega)$ for surface waves driven by a vertical vibration of the vessel. Our computations are performed for the ferrofluid EMG 909 (Ferrofluidics Corporation), which has been used in recent experiments [5,6,9]. The fluid parameters are $\nu=6$ mm^2/s, $\rho=1.02$ g/cm^3, $\gamma=0.0265$ N/m, and $\chi=0.8$. To achieve a dispersion with a considerable hysteresis a static magnetization $M_G=0.99\times M_R$ is imposed. Figure 3 depicts some representative neutral stability curves for the subharmonic Faraday resonance at different values of the drive frequency and the filling level h. The harmonic instability tongue is suppressed as it always leads to a higher threshold within the considered parameter range. Depending on the excitation frequency the neutral curves in Fig. 3 exhibit up to three local minima, which reflect the three branches of the hysteretic dispersion shown in Fig. 2. The first row in Fig. 3 with $h=10$ cm represents the infinite depth limit. In this case dissipation is solely dominated by viscous friction in the bulk flow, which is proportional to νk^2. At small drive frequencies [Figs. 3(a) and 3(b)] the critical wave number k_S is determined by the left local minimum, which corresponds to the dispersion branch (i) in Fig. 2. At the filling level $h=5$ mm [Figs. 3(d)–3(f)] dissipation in the bottom boundary layer becomes important below k

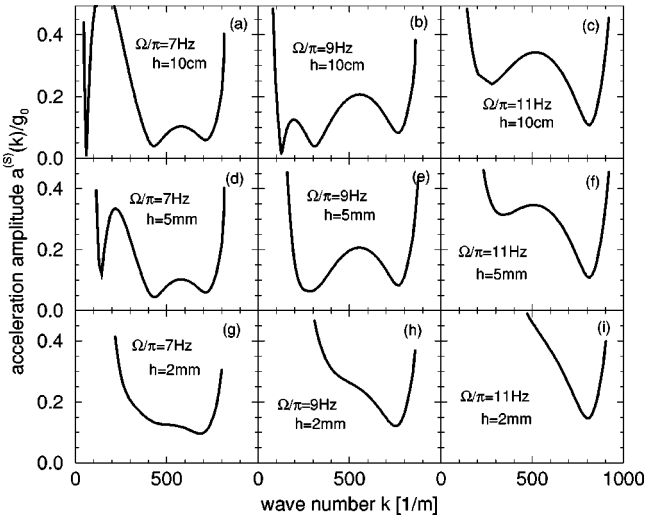

FIG. 3. Neutral stability curve $a^{(S)}(k)$ for the subharmonic Faraday instability at different drive frequencies Ω and filling levels h. The applied magnetization M_G is 1% below the Rosensweig threshold M_R for a deep fluid layer. Below (above) the resonance tongues the plane surface is stable (unstable). The absolute minimum of the neutral curve determines the critical wave number k_S and the onset amplitude $a_c^{(S)}$. Parameters as in Fig. 2.

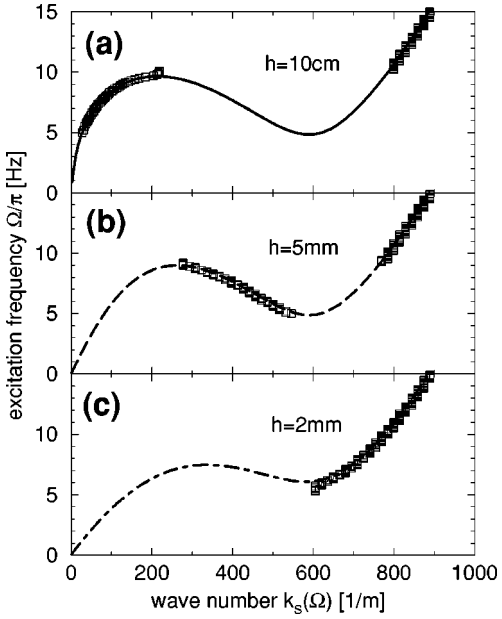

FIG. 4. The dispersion of *parametrically driven* surface waves at different filling levels h as obtained from the eigenvalue problem Eq. (3.9) (squares). For the sake of comparison, the dispersion for *free inviscid* surface waves [according to Eq. (3.2) and shown in Fig. 2] is presented as a line. Parameters as in Fig. 2.

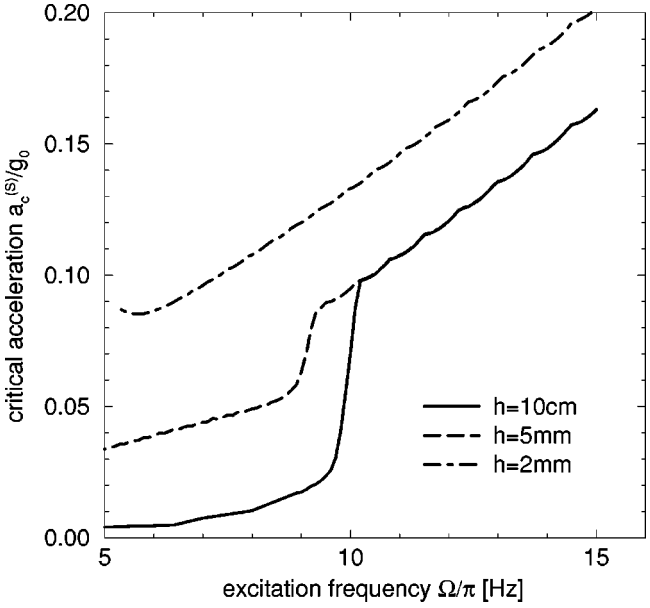

FIG. 5. The critical acceleration amplitude $a_c^{(S)}$ for the onset of subharmonic Faraday waves. Parameters as in Fig. 2.

$\sim 1/h = 200\ \mathrm{m}^{-1}$. Wave numbers in that region are strongly damped and their onset is delayed. The absolute minimum of the marginal curve in Figs. 3(d)–3(e) is thus selected from the anomalous dispersion branch (ii). On reducing h even further, an increasing wave number range is eliminated from the spectrum of available modes. At $h = 2$ mm [Figs. 3(g)–3(i)] wave numbers below $k \sim 1/h = 500\ \mathrm{m}^{-1}$ are strongly inhibited and thus k_S is always located on the normal dispersion branch (iii).

Figure 4 shows the critical wave number $k_S(\Omega)$ as obtained by minimizing the neutral curves with respect to k. As damping is weak the computed dispersion for parametrically driven waves (indicated by squares) compares well with the inviscid relation $\omega_0(k)$ (lines). Depending on the filling level h, the normal as well as the anomalous branches can be probed. Wave number jumps occur when two neighboring minima in the neutral chart appear at the same drive amplitude a. Such a coexistence of two unstable wave numbers occurs in Figs. 4(a) and 4(b) at a drive frequency of $\Omega/\pi \simeq 10$ Hz. Recently, supercritical ''twin peak'' patterns have been observed [6] at an excitation frequency of 9.6 Hz. They are likely the result of this bicriticality. The observed wave number ratio of approximately 4 must be compared with the value ~ 3, which can be read off from Fig. 4(b). Note however, that the experiment is performed in a narrow channel, while the present analysis is made for a laterally infinite layer. By carefully tuning both the drive frequency and the filling level, it is possible to achieve a tricritical situation, where all three minima of the neutral curve (Fig. 3) occur at the same acceleration amplitude.

We mention that the linear dispersion $k_S(\Omega)$ calculated here need not coincide with the wave number of relaxed nonlinear wave patterns [6]. Nevertheless, our prediction should at least be measurable during the transient growth of a perturbation out of the unstable plane surface.

Even though viscous dissipation does not appreciably enter the dispersion $k_S(\Omega)$, it is crucial for the threshold amplitude $a_c^{(S)}(\Omega)$. Figure 5 depicts the corresponding theoretical prediction. The steep steps in the curves for $h = 10$ cm and $h = 5$ mm are related to the wave number jumps in Figs. 4(a) and 4(b). No bicriticality occurs at the level $h = 2$ mm.

Within the low viscosity limit $\nu k^2/\Omega \ll 1$ an approximative expression for the onset amplitude can be computed. A perturbative expansion analogous to Ref. [14] leads to

$$a_c^{(S)} \simeq \frac{2\Omega^2}{k_S} \mathrm{Im}[X(k_S,\Omega)] \coth(k_s h), \tag{4.1}$$

where Im denotes the imaginary part. On ignoring viscous corrections to the dispersion, k_S can be evaluated by solving the transcendent equation $\Omega = \omega_0(k_s)$. Among the possible roots, take that one which yields the smallest value of $a_c^{(S)}$.

B. Bicriticality of Faraday and Rosensweig instability

The theory of the Mathieu oscillator reveals that the stable equilibrium position of a pendulum can be destabilized by a gravity modulation. This is the basic mechanism of the Faraday instability. However, it is also known that the unstable equilibrium of the pendulum (upright position) can be stabilized by the same parametric drive. It is therefore tempting to transfer this idea to hydrodynamic systems. This has been successfully demonstrated for Rayleigh Bénard convection [16,17], where the supercritical conductive state could be stabilized by a modulation of the applied temperature gradient. Likewise one expects that the Rosensweig instability in ferrofluids can also be delayed or suppressed by the gravity modulation. Figure 6 shows the neutral stability diagram for three different drive frequencies at a magnetic field amplitude which exceeds the Rosensweig threshold by 0.5%. The upper instability tongue is related to the subharmonic Fara-

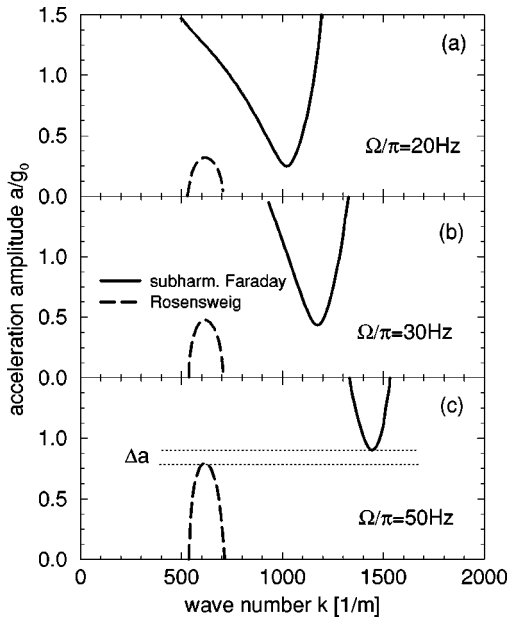

FIG. 6. The neutral stability curves for the subharmonic Faraday instability (solid line) and the Rosensweig instability (dashed line) at different drive frequencies. The magnetization M_G is 0.5% *higher* than the Rosensweig threshold M_R. At $\Omega/\pi=50$ Hz the rest state (plane surface) is linearly stable for drive amplitudes within the gap Δa. Fluid parameters for EMG 909, $h=5$ mm.

day resonance already presented in Fig. 3. The new tongue entering the stability diagram form below corresponds to the Rosensweig instability. If Ω is high enough [Fig. 6(c)] Faraday and Rosensweig tongues do not overlap on the a axis. Drive amplitudes within the gap Δa stabilize the basic plane surface state. On leaving the gap towards larger a, Faraday waves will be excited, while a reduction of a below the gap leads to the onset of the Rosensweig instability. Figure 7 shows the threshold of both instabilities as a function of the static field strength H_G and the excitation frequency Ω/π. The stable gap can be increased by either decreasing the magnetic field strength (the Rosensweig tongue withdraws) or by increasing the vibration frequency (the Faraday threshold rises). The critical wave number $k_R\sim 614$ m^{-1}, which belongs to the maximum of the Rosensweig tongue, is almost independent of H_G and Ω. This is in contrast to the critical Faraday wave number k_S, which depends strongly on Ω via the dispersion [cf. inset in Fig. 7(b)]. The two instabilities also distinguish by the time dependence of the excited waves: Faraday waves oscillate subharmonically around a zero mean value [$\beta=1$ in Eq. (3.8)]. On the other hand, waves beyond the Rosensweig onset oscillate around a finite mean value synchronously to the external drive. In light of Eq. (3.8) they belong to the subclass of waves with $\beta=0$.

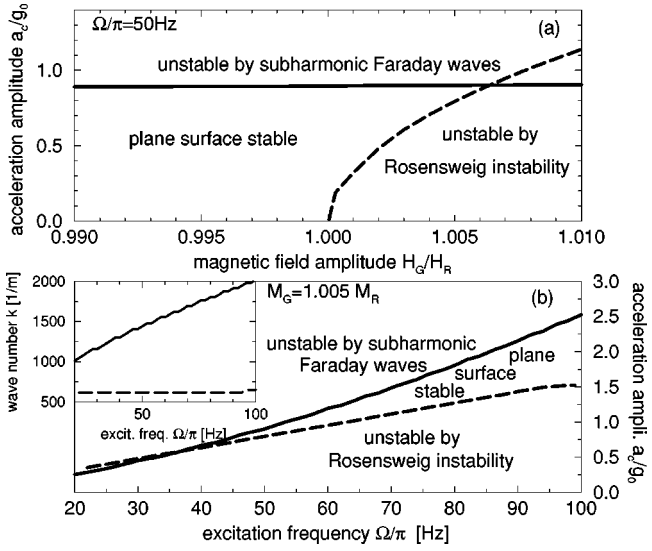

FIG. 7. The stability thresholds for subharmonic Faraday waves (solid line) and the Rosensweig instability (dashed line) as a function of (a) the applied magnetic field H_G or (b) the excitation frequency Ω/π. The magnetic field is measured in units of H_R. Parameters as in Fig. 2, $h=5$ mm.

Mediated by quadratic nonlinearities in the hydrodynamic equations a coupling among three Rosensweig modes occurs if their lateral wave vectors fulfill the geometric resonance condition $\mathbf{k}_{R1}+\mathbf{k}_{R2}=\mathbf{k}_{R3}$, where $|\mathbf{k}_{Ri}|=k_R$. This is the generic triad wave vector interaction which enforces hexagonal surface patterns [1]. An analogous resonance among three Faraday modes is inhibited by the subharmonic symmetry of their time dependence. Those Faraday patterns usually exhibit a square symmetry, which results from a four-wave vector interaction [19].

The existence of a Faraday-Rosensweig bicriticality opens the possibility for a nonlinear cross coupling between two Faraday modes, k_{S1} and k_{S2}, and one Rosensweig mode k_R. Temporal as well as spatial resonance is ensured if $\mathbf{k}_{S1}+\mathbf{k}_{S2}=\mathbf{k}_R$ holds. The angle ϕ between $\mathbf{k}_{S1}$ and $\mathbf{k}_{S2}$ depends on $|\mathbf{k}_S|$ and can be controlled by the excitation frequency Ω [see inset of Fig. 7(b)]. Thus pattern formation can be influenced by varying this external control parameter. By inspection it can be seen that the combined action of self- and cross-coupling between the different modes takes maximum advantage if the angle ϕ is tuned to be 150°. This corresponds to

$$k_S=k_R/\sqrt{2(1+\cos\phi)}\simeq 614\ \text{m}^{-1}/\sqrt{2[1+\cos(150°)]}$$
$$\simeq 1190\ \text{m}^{-1}. \tag{4.2}$$

In this case, quasiperiodic surface patterns with a twelve-fold orientational symmetry are likely to occur. Recently, this resonant coupling was shown [15] to enforce quasiperiodic structures in Rayleigh-Bénard convection under gravity modulation. Clearly, the above simple resonance argument does not replace a full nonlinear calculation; nevertheless, it is a strong indicator and at least a hint at an interesting parameter regime. For the fluid EMG 909 (depth $h=5$ mm) we find that the appropriate bicriticality appears at $M_G\simeq 1.004\times M_R$ and $\Omega/\pi\simeq 32$ Hz.

V. DISCUSSION

The experiments presented in Refs. [5,6] have been performed in a narrow ring channel of 5 mm width. This confined geometry is presumably inappropriate for a quantitative comparison with the above results. For instance, the strong deviations between the empiric Rosensweig wave number and the theoretical value $k_R=\sqrt{\rho g_0/\gamma}$ are suspected to arise from the container side walls and inhomogeneities of the

magnetic field. Measurements in a container with a larger horizontal extension are thus desirable. Other problems usually encountered with water- or kerosin-based ferrofluids (EMG909 belongs to this class) are the evaporation of the solvent and a drift of the surface tension due to contamination. Here, oil based ferrofluids are more appropriate. Those fluids are less sensitive against surface impurities. Moreover, since they are also more viscous, parasitic damping effects due to the container side walls and the meniscus contact line [18,19] would become less disturbing. Recent Faraday experiments [20,21] with (nonmagnetic) silicone-oils as working fluids demonstrate that empiric onset data and theoretical predictions coincide within a few percent.

In this paper surface waves are investigated, which are driven by a periodic modulation of gravity. Alternatively, a modulation of the applied magnetic field could be used according to $H_G = H_{G0} + a\cos(2\Omega t)$. In this case the basic state magnetization $M_G(t) = \chi H_G(t)$ becomes time dependent. As it enters *quadratically* into Eq. (3.2), the effective excitation signal is composed of two frequencies, except in the limit $a \ll H_{G0}$. It should also be noticed that the effective magnetic drive is proportional to k^2 while it is linear in k for the gravity modulation. Shorter wavelengths are thus favored by the magnetic drive. This effect might be important in a recent magnetic Faraday experiment [9], where the first members of the alternating subharmonic-harmonic resonant cascade have been observed. This succession has been predicted [22] (for nonmagnetic liquids), when the experiment is operated in the so-called lubrication limit, where h compares to the viscous skin depth $\sqrt{\nu/\Omega}$. In this situation, however, the phenomenon of rotational viscosity in ferrofluids can no longer be ignored. While the flow field in thick layers can be considered irrotational, this approximation fails in the lubrication limit. The flow in thin layers is predominately vortical and the finite magnetic relaxation time leads to an increased effective viscosity [23]. The additional contribution might be detectable in a careful measurement of the onset threshold, which in turn depends sensitively on the viscous dissipation.

ACKNOWLEDGMENTS

Stimulating discussions with M. Lücke, T. Mahr, I. Rehberg, and R. Richter are appreciated. Support by the Deutsche Forschungsgemeinschaft through the SFB 277 is gratefully acknowledged.

[1] R. E. Rosensweig, *Ferrohydrodynamics* (Cambridge University Press, Cambridge, 1993).
[2] B. M. Berkovski, V. F. Medvedev, and M. S. Krakov, *Engineering Applications* (Oxford Science Publications, New York, 1993).
[3] E. Blums, A. Cebers, and M. Maiorov, *Magnetic Fluids* (de Gruyter, Berlin, (1997).
[4] M. D. Cowley and R. E. Rosensweig, J. Fluid Mech. **30**, 671 (1967).
[5] T. Mahr, A. Groisman, and I. Rehberg, J. Magn. Magn. Mater. **159**, L45-L50 (1996).
[6] B. Reimann, T. Mahr, R. Richter, and I. Rehberg, J. Magn. Magn. Mater. (to be published).
[7] R. E. Zelazo and J. R. Melcher, J. Fluid Mech. **39**, 1 (1969).
[8] V. G. Bashtovoi and R. E. Rosensweig, J. Magn. Magn. Mater. **122**, 234 (1993); there is a misprint in their Eq. (A12).
[9] T. Mahr and I. Rehberg, Europhys. Lett. **43**, 23 (1998).
[10] J. C. Bacri, A. Cebers, J. C. Dabadie, S. Neveu, and R. Perzynski, Europhys. Lett. **27**, 437 (1994); J. C. Bacri, A. Cebers, J. C. Dabadie, and R. Perzynski, Phys. Rev. E **50**, 2712 (1994).
[11] J. Weilepp and H. R. Brand, J. Phys. II **6**, 419 (1996).
[12] B. Abou, G. N. de Surgy, and J. E. Wesfreid, J. Phys. II **7**, 1159 (1997).
[13] K. Kumar and L. S. Tuckerman, J. Fluid Mech. **279**, 49 (1994); K. Kumar, Proc. R. Soc. London, Ser. A **452**, 1113 (1996).
[14] H. W. Müller, H. Wittmer, C. Wagner, J. Albers, and K. Knorr, Phys. Rev. Lett. **78**, 2357 (1993).
[15] S. H. Davis, Annu. Rev. Fluid Mech. **8**, 57 (1976) and cited references.
[16] G. Ahlers, P. C. Hohenberg, and M. Lücke, Phys. Rev. A **32**, 3519 (1985).
[17] S. T. Milner, J. Fluid Mech. **225**, 81 (1991).
[18] U. Volmar and H. W. Müller, Phys. Rev. E **56**, 5423 (1997).
[19] J. W. Miles, Proc. R. Soc. London, Ser. A **297**, 459 (1967).
[20] J. Bechhoefer, V. Ego, S. Manneville, and B. Johnson, J. Fluid Mech. **288**, 325 (1995).
[21] B. Christiansen, P. Alstrom, and L. Levinsen, J. Fluid Mech. **291**, 323 (1995).
[22] E. Cerda and E. Tirapegui, Phys. Rev. Lett. **78**, 859 (1997).
[23] M. J. Shliomis, Zh. Éksp. Teor. Fiz. **61**, 2411 (1971) [Sov. Phys. JETP **34**, 1291 (1972)].